Fourier Transform Infrared Spectroscopy

C.C. Homes*
Condensed Matter Physics & Materials Science Department
Brookhaven National Laboratory
Upton, NY 11973

May 16, 2011

*These notes are adapted from a set of informal lectures developed by my thesis advisor, Prof. J. E. Eldridge, Department of Physics & Astronomy, University of British Columbia, Vancouver, B.C., Canada.

Contents

1 Fourier Transform Spectroscopy **3**

1.1 Polychromatic source 4

1.1.1 Percentage modulation 5

1.2 Fourier transform 6

1.3 Double-sided interferogram 6

1.3.1 Complex Fourier transform 7

1.4 Finite integration limits 9

1.4.1 The convolution theorem 9

1.4.2 Resolution 11

1.5 Apodisation 12

1.5.1 Resolution revisited 13

1.6 Sampling interval 15

1.6.1 The Shah function 15

1.7 Felgett advantage ("Multiplex") 18

1.8 Relating (S/N) in the interferogram to (S/N) in the spectrum 20

2 Instrumentation **21**

2.1 Self-supporting dielectric beam splitters 21

2.1.1 Efficiency of a dielectric beamsplitter with frequency 21

2.1.2 Relating $\boldsymbol{\delta}$ to $\bar{\boldsymbol{\nu}}$ 23

2.2 Polarization in Mylar beam splitters 25

A Optical Conductivity **27**

1 Fourier Transform Spectroscopy

Since its inception, most interferometer designs have incorporated some element of a basic Michelson interferometer, shown schematically in Figure 1. Both beams have been transmitted once and reflected once as they are divided at the beamsplitter, then reflected at either the movable (M1) or fixed (M2) mirror, and finally recombined at the beam splitter to proceed to the sample area and the detector.

Consider an incoming monochromatic plane wave with an average electric field amplitude E_m, frequency ω and wave number $\bar{\nu}$ (which as units of cm^{-1}):

$$\bar{\nu} = \frac{1}{\lambda} = \frac{\omega}{2\pi c} \tag{1}$$

(where λ is in cm), incident on the beam splitter (where c is the speed of light)

$$\vec{E} = \vec{E}_m \cos(\omega t - 2\pi\bar{\nu}y). \tag{2}$$

The beam from the mirror M2 after leaving the beam splitter in the direction of the condensing unit may be written as

$$\vec{E}_2 = rtc\vec{E}_m \cos\left[\omega t - 2\pi\bar{\nu}y_1\right] \tag{3}$$

where r is the reflectance (amplitude) of the beam splitter, t is the transmittance, and c is a constant depending on the polarization. Similarly from the other mirror M1, at the same point then we have

$$\vec{E}_2 = rtc\vec{E}_m \cos\left[\omega t - 2\pi\bar{\nu}(y_1 + x)\right] \tag{4}$$

where x is the path difference. By superimposing (or superposition), the resultant E is given by

$$\vec{E}_R = \vec{E}_1 + \vec{E}_2 = 2rtc\vec{E}_m \cos(\omega t - 2\pi y_1)\cos(\pi\bar{\nu}x). \tag{5}$$

The intensity (I) detected is the time average of E^2. More strictly $\vec{E} \times \vec{H}$ (the Poynting vector), but because $|\vec{E}| \propto |\vec{H}|$ this quantity can be described simply by just $|\vec{E}|$, neglecting some constant of proportionality (which is not important). The intensity may be written as:

$$I \propto 4r^2t^2c^2E_m^2 \cos^2(\omega t - 2\pi y_1\bar{\nu})\cos^2(\pi\bar{\nu}x) \tag{6}$$

where the time average of the first cosine term is just $1/2$. Thus

$$I \propto 2I(\bar{\nu})\cos^2(\pi\bar{\nu}x), \tag{7}$$

where $I(\bar{\nu})$ is a constant that depends only upon $\bar{\nu}$. This expression may be simplified to

$$I(x) = I(\bar{\nu})[1 + \cos(2\pi\bar{\nu}x)] \tag{8}$$

where $I(x)$ is the *interferogram* form a monochromatic source. The interferogram for a monochromatic source is shown in Fig. 2.

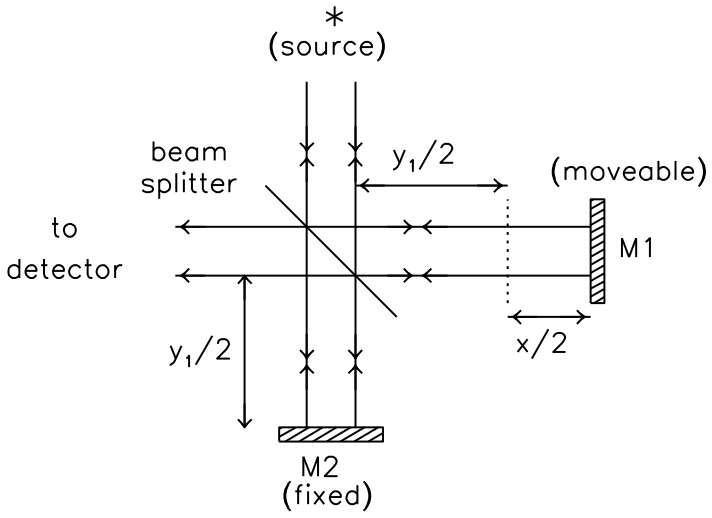

Figure 1: A schematic view of a simple Michelson interferometer. The beam from the source (typically a Hg arc lamp) is collimated and the wavefront is divided at the beam splitter. One arm of the interferometer consists of a fixed mirror, while the other arm contains a moveable mirror. The beams are recombined at the beam splitter after having been reflected once and transmitted once, and then proceed to the sample area and detector.

1.1 Polychromatic source

One of the advantages of the Fourier transform instrument is that many different wave numbers may be looked at simultaneously — all the information is gathered at the same time, and we sort it all out using a Fourier transform later. This decreases the measurement time. As well, we can have much more "thruput", i.e. higher intensities and larger solid angles. An interferogram for a polychromatic source which consists of frequencies from $0 \rightarrow \bar{\nu}_m$ is thus:

$$\begin{aligned} I(x) &= \int_0^{\bar{\nu}_m} I(\bar{\nu})[1+\cos(2\pi\bar{\nu}x)]d\bar{\nu} \\ &= \int_0^{\bar{\nu}_m} I(\bar{\nu})d\bar{\nu} + \int_0^{\bar{\nu}_m} I(\bar{\nu})\cos(2\pi x)dx. \end{aligned} \tag{9}$$

When $x = 0$ then

$$\begin{aligned} I(0) &= 2\int_0^{\bar{\nu}_m} I(\bar{\nu})d\bar{\nu} \\ \Rightarrow I(x) &= \frac{1}{2}I(0) + \int_0^{\bar{\nu}_m} I(\bar{\nu})\cos(2\pi\bar{\nu}x)d\bar{\nu}. \end{aligned} \tag{10}$$

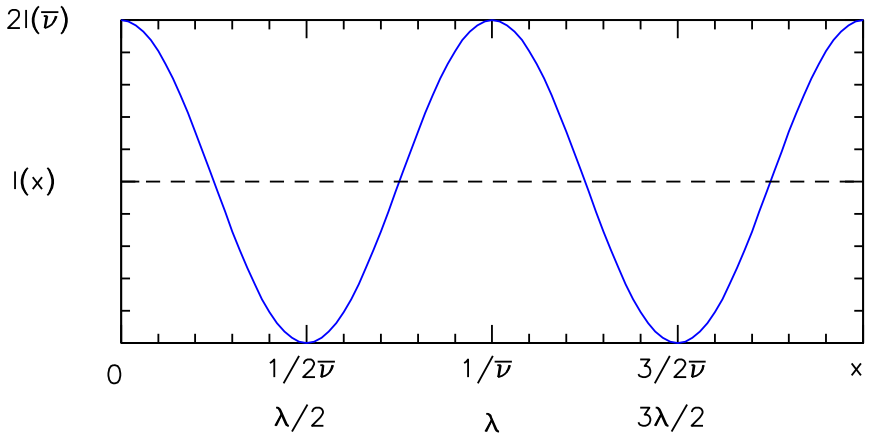

Figure 2: The interference pattern for a monochromatic source (such as a laser) as a function of mirror displacement.

With many different wave lengths present, the interferogram resembles the diagram in Fig. 3, which is symmetrical about $x = 0$ for an ideal interferogram.

When $x = 0$ the interference between all of the frequencies is constructive, resulting in a central maxima. However, for $x = \infty$ the frequencies add both constructively and destructively, so that the net contribution due to the integral in Eq. 10 is simply zero. Thus,

$$I(\infty) = \frac{1}{2} I(0) \tag{11}$$

or more simply, $I(0) = 2I(\infty)$. This relationship is an important check of the instrument alignment.

1.1.1 Percentage modulation

The percentage of modulation is defined as

$$\frac{[I(0) - I(\infty)]}{I(\infty)} \times 100 \tag{12}$$

In a well-aligned instrument, the modulation is $> 85\%$, and this value should be $> 95\%$ in the low frequency region.

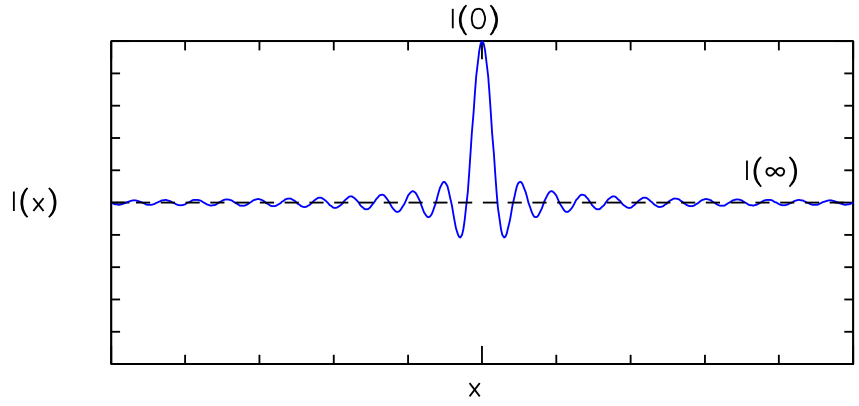

Figure 3: The interference pattern for a polychromatic source about the zero path difference. This curve was generated simply by taking the normalized sum of a number of cosine functions with various frequencies. Note that $I(0) = 2I(\infty)$.

1.2 Fourier transform

We have $I(x)$ and now want $I(\bar{\nu})$, i.e.:

$$I(x) - I(\infty) = \int_0^{\bar{\nu}_m} I(\bar{\nu}) \cos(2\pi\bar{\nu}x) d\bar{\nu} \tag{13}$$

letting $\bar{\nu}_m \to \infty$, we can write

$$I(\bar{\nu}) = \int_0^{\infty} [I(x) - I(\infty)] \cos(2\pi\bar{\nu}x) dx. \tag{14}$$

This procedure involves sampling each position, which can take a long time if the signal is small and the number of frequencies being sampled is large.

1.3 Double-sided interferogram

If $F(x) = I(x) - I(\infty)$, then

$$F(x) = \int_0^{\bar{\nu}_m} I(\bar{\nu}) \cos(2\pi\bar{\nu}x) d\bar{\nu} \tag{15}$$

is symmetric about $x = 0$ since cosine is an even function. However, what if the interferogram behaves differently for $-x$ and $+x$; i.e. you have not sampled at the true zero path difference.

Loss of symmetry can be represented by an additional phase factor:

$$F(x) = \int_0^{\bar{\nu}_m} I(\bar{\nu}) \cos\left[2\pi\bar{\nu}x - \phi\right] d\bar{\nu} \tag{16}$$

$$= \int_0^{\bar{\nu}_m} I(\bar{\nu}) \cos\phi \cos(2\pi\bar{\nu}x) d\bar{\nu} + \int_0^{\bar{\nu}_m} I(\bar{\nu}) \sin\phi \sin(2\pi\bar{\nu}x) d\bar{\nu}. \tag{17}$$

What we would like to do is to find a method to be able to deal with the problem of not being at the true zero path difference. For this, we use the complex Fourier transform.

1.3.1 Complex Fourier transform

The complex Fourier transform is defined in the following way:

$$g(\bar{\nu}) = \int_{-\infty}^{\infty} f(x) e^{2\pi i\bar{\nu}x} dx$$

$$= \int_{-\infty}^{\infty} f(x) \cos(2\pi\bar{\nu}x) dx + i \int_{-\infty}^{\infty} f(x) \sin(2\pi\bar{\nu}x) dx. \tag{18}$$

The inverse transform is given by

$$f(x) = \int_{-\infty}^{\infty} g(\bar{\nu}) e^{-2\pi i\bar{\nu}x} d\bar{\nu}$$

$$= \int_{-\infty}^{\infty} g(\bar{\nu}) \cos(2\pi\bar{\nu}x) d\bar{\nu} - i \int_{-\infty}^{\infty} g(\bar{\nu}) \sin(2\pi\bar{\nu}x) d\bar{\nu}. \tag{19}$$

If $f(x)$ is even, $[f(x) = f(-x)]$ then

$$g(\bar{\nu}) = \int_{-\infty}^{\infty} f(x) \cos(2\pi\bar{\nu}x) dx$$

$$= 2\int_0^{\infty} f(x) \cos(2\pi\bar{\nu}x) dx. \tag{20}$$

This is referred to as a *cosine transform*. Likewise, if $f(x)$ is odd, then

$$g(\bar{\nu}) = i\int_{-\infty}^{\infty} f(x) \sin(2\pi\bar{\nu}x) dx$$

$$= 2i\int_0^{\infty} f(x) \sin(2\pi\bar{\nu}x) dx, \tag{21}$$

is a *sine transform*. Thus, we write

$$g(\bar{\nu}) = C(\bar{\nu}) + iS(\bar{\nu}). \tag{22}$$

Returning to the problem of the interferogram, let $F(x) \equiv f(x)$, [which is $I(x) - I(\infty)$]. then

$$\begin{aligned} C(\bar{\nu}_1) &= \int_0^{\bar{\nu}_m} I(\bar{\nu}) \cos\phi \left[\int_{-\infty}^{\infty} \cos(2\pi\bar{\nu}x) \cos(2\pi\bar{\nu}_1 x) dx \right] d\bar{\nu} \\ &\quad + \int_0^{\bar{\nu}_m} I(\bar{\nu}) \sin\phi \left[\int_{-\infty}^{\infty} \sin(2\pi\bar{\nu}x) \sin(2\pi\bar{\nu}_1 x) dx \right] d\bar{\nu}. \end{aligned} \tag{23}$$

Now,

$$\begin{aligned} \int_{-\infty}^{\infty} \cos(2\pi\bar{\nu}x) \cos(2\pi\bar{\nu}_1)x) dx &= \frac{1}{2} \int_{-\infty}^{\infty} \left[e^{2\pi i(\bar{\nu}+\bar{\nu}_1)x} + e^{2\pi i(\bar{\nu}-\bar{\nu}_1)x} \right] dx \\ &= \frac{1}{2} \left[\delta(\bar{\nu} + \bar{\nu}_1) + \delta(\bar{\nu} - \bar{\nu}_1) \right]. \end{aligned} \tag{24}$$

where δ is the Dirac δ function. Note that the sine terms go to zero in the integral when the limits are from $-\infty \to \infty$. This is of the form

$$\delta(\bar{\nu} + L) = \int_{-\infty}^{\infty} e^{2\pi i(\bar{\nu}+L)x} dx \tag{25}$$

In the expression for $C(\bar{\nu}_1)$ we have the product of a sine and a cosine in the interior of the second integral. However, as the sine is a odd function, then its value over the range $-\infty \to \infty$ will be zero. Thus, we can write $C(\bar{\nu}_1)$ as

$$\begin{aligned} C(\bar{\nu}_1) &= \frac{1}{2} \int_0^{\bar{\nu}_m} I(\bar{\nu}) \cos\phi \left[\delta(\bar{\nu} + \bar{\nu}_1) + \delta(\bar{\nu} - \bar{\nu}_1) \right] d\bar{\nu} \\ \Rightarrow C(\bar{\nu}_1) &= \frac{I(\bar{\nu}_1}{2} \cos\phi; \quad I(-\bar{\nu}_1) = 0. \end{aligned} \tag{26}$$

since $I(\bar{\nu}) = 0$ for all $\bar{\nu} > \bar{\nu}_m$ and for all $\bar{\nu} < 0$. Similarly,

$$S(\bar{\nu}_1) = \frac{I(\bar{\nu}_1)}{2} \sin\phi. \tag{27}$$

Thus

$$\begin{aligned} |g(\bar{\nu}_1)| &= \left[C^2(\bar{\nu}_1) + S^2(\bar{\nu}_1) \right]^{1/2} \\ &= \frac{1}{2} I(\bar{\nu}_1) (\sin^2\phi + \cos^2\phi)^{1/2} \\ &= \frac{I(\bar{\nu}_1)}{2} \end{aligned}$$

so that finally

$$\begin{aligned} I(\bar{\nu}_1) &= 2|g(\bar{\nu}_1)| \\ &= 2\left[C^2(\bar{\nu}_1) + S^2(\bar{\nu}_1)\right]^{1/2} \end{aligned} \tag{28}$$

Thus, the phase error introduced by not sampling symmetrically and the asymmetry in the interferometer is eliminated by taking the the two-sided interferogram and performing a complex fast Fourier transform.

Disadvantages: a factor of two in the data collection time, because the interferogram must be two sided.

1.4 Finite integration limits

In practice the interferogram is from $-x_{max}$ to $+x_{max}$, not $-\infty$ to ∞. To examine the effect, consider the *monochromatic* wave in an ideal interferometer. From Eqs. 6 or 13 (neglecting the constant offset) we get

$$F(x) = I(\bar{\nu}_1)\cos(2\pi\bar{\nu}_1 x) \tag{29}$$

where $F(x)$ is just the structure. We can do the finite transform over the finite range, which may be written as:

$$\int_{-\infty}^{\infty} I(\bar{\nu}_1)\cos(2\pi\bar{\nu}_1 x)e^{2\pi i\bar{\nu}x}\mathrm{rect}(x)dx \tag{30}$$

which is to say that instead of putting limits on the integral, we use the rectangular function defined by:

$$\mathrm{rect}(x) = \begin{cases} 1 & |x| < x_{max} \\ 0 & |x| > x_{max} \end{cases}$$

1.4.1 The convolution theorem

The Fourier transform of the product of two functions, i.e. $f(x)$ and $g(x)$ is the convolution of their individual Fourier transforms $F(y)$ and $G(y)$, where the convolution is defined by

$$F * G = \int_{-\infty}^{\infty} G(u)F(y-u)du \tag{31}$$

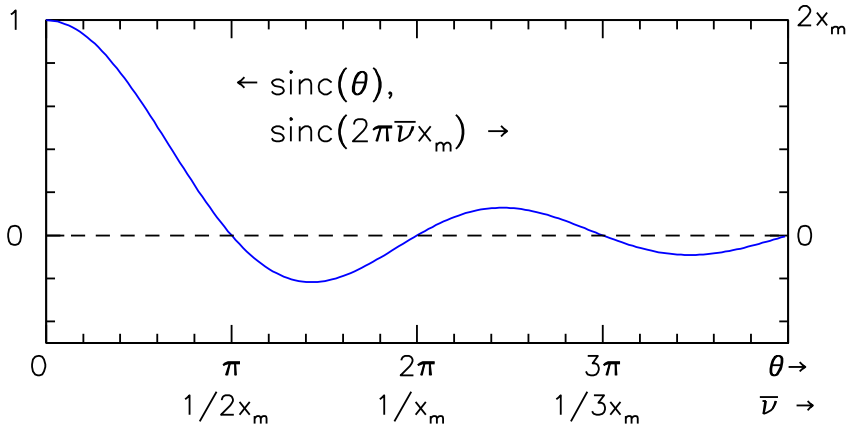

Figure 4: The function $\mathrm{sinc}(\theta)$ for the rectangular aperture function.

The Fourier transform of $\mathrm{rect}(x)$ is then

$$\begin{aligned}
\int_{-\infty}^{\infty} \mathrm{rect}(x) e^{2\pi i \bar{\nu} x} dx &= \int_{-x_m}^{x_m} e^{2\pi i \bar{\nu} x} dx \\
&= \int_{-x_m}^{x_m} \left[\cos(2\pi\bar{\nu}x) + i\sin(2\pi\bar{\nu}x)\right] dx \\
&= \left[\frac{\sin(2\pi\bar{\nu}x)}{2\pi\bar{\nu}} - i\frac{\cos(2\pi\bar{\nu}x)}{2\pi\bar{\nu}}\right]_{-x_m}^{x_m} \\
&= \frac{2\sin(2\pi\bar{\nu}x_m)}{2\pi\bar{\nu}} \\
&= 2x_m \frac{\sin(2\pi\bar{\nu}x_m)}{2\pi\bar{\nu}x_m} \\
&= 2x_m \mathrm{sinc}(2\pi\bar{\nu}x_m). \qquad (32)
\end{aligned}$$

This function is shown in Fig. 4. The Fourier transform of the structure $F(x)$ due to the monochromatic source is:

$$\begin{aligned}
\int_{-\infty}^{\infty} I(\bar{\nu}_1)\cos(2\pi\bar{\nu}_1 x) e^{2\pi i \bar{\nu} x} dx &= \frac{1}{2}\int_{-\infty}^{\infty} I(\bar{\nu}_1)\left[e^{2\pi i\bar{\nu}x} + e^{-2\pi i\bar{\nu}_1 x}\right] e^{2\pi i\bar{\nu}_1 x} dx \\
&= \frac{1}{2}\int_{-\infty}^{\infty} I(\bar{\nu}_1)\left[e^{2\pi i(\bar{\nu}+\bar{\nu}_1)x} + e^{2\pi i(\bar{\nu}-\bar{\nu}_1)x}\right] dx \\
&= \frac{1}{2} I(\bar{\nu}_1)\left[\delta(\bar{\nu}+\bar{\nu}_1) + \delta(\bar{\nu}-\bar{\nu}_1)\right] \qquad (33)
\end{aligned}$$

This function is simply two delta functions located at $\pm\bar{\nu}_1$. We usually discard the the negative frequency as it is unphysical, thus we are simply left with the frequency $\bar{\nu}_1$ of the monochromatic source.

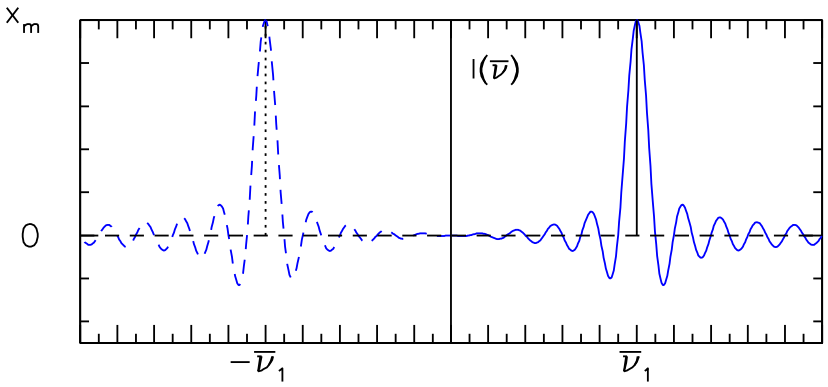

Figure 5: The convolution of the delta function from a single monochromatic source at $\pm\bar{\nu}_1$ and a rectangular aperture function. While the response from the negative side extends into the positive region, it is usually very small and it is ignored. Note that the Fourier transform of the rectangular aperture function is called the instrumental line shape (ILS).

The convolution theorem of two transforms is then:

$$\begin{aligned} & \int_{-\infty}^{\infty} 2x_m \mathrm{sinc}(2\pi u x_m) \frac{1}{2} I(\bar{\nu}) \left[\delta(\bar{\nu}+\bar{\nu}_1+u) + \delta(\bar{\nu}-\bar{\nu}_1+u)\right] du \\ = \;& I(\bar{\nu}_1) x_m \left\{\mathrm{sinc}[2\pi(\bar{\nu}+\bar{\nu}_1)x_m] + \mathrm{sinc}[2\pi(\bar{\nu}-\bar{\nu}_1)x_m]\right\} \end{aligned} \tag{34}$$

which is shown in Figure 5.

The total from the negative side extends into the positive region, but is usually very small and ignored. Thus:

$$I(\bar{\nu}) = I(\bar{\nu}_1) x_m \mathrm{sinc}[2\pi(\bar{\nu}-\bar{\nu}_1)x_m]. \tag{35}$$

The function $2x_m\mathrm{sinc}(2\pi\bar{\nu}x_m)$ is called the *instrumental line shape* (ILS) or the *spectral window*.

$$I(\bar{\nu}) = I(\bar{\nu}_1) * \mathrm{ILS}. \tag{36}$$

1.4.2 Resolution

Clearly, the ILS has a given width for a monochromatic line. Jacquinot defined the resolution as the distance between the first two zeros on either side of the peak, which is shown in Figure 6 for a sinc function.

Thus,

$$\delta_{\bar{\nu}} = \frac{1}{x_m}. \tag{37}$$

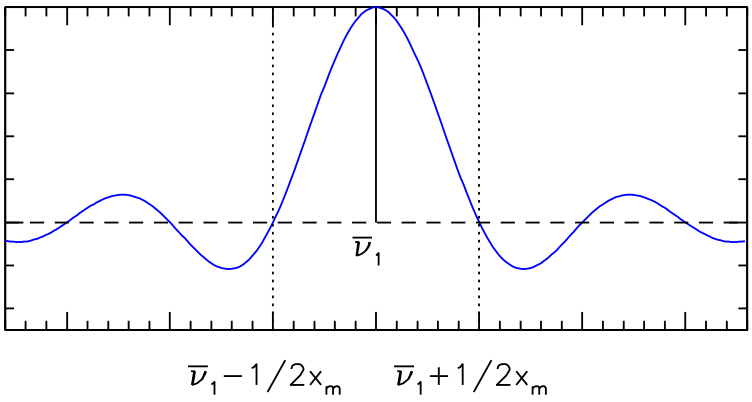

Figure 6: The first two zeros of a sinc function, which occur at $\bar{\nu}_1 \pm 1/2x_m$.

(Note that this delta function is not the Dirac delta function.) Thus, the resolution depends on the length of the scan, i.e. if the mirror scan is 5 cm (which is $x_m/2$), then $x_m = 10$ cm, $\Rightarrow \delta_{\bar{\nu}} = 0.1$ cm^{-1}.

1.5 Apodisation

The "side lobes" or "feet" of the sinc function drop off 22% below zero, which is clearly unacceptable. The problem is in choosing the aperture. The sharp edges produced by the rectangular function introduce this ringing in the spectrum. Thus, what we need is a gentler aperture function. The imposition of such a function is called *apodisation*. The most common apodisation function is the triangular aperture, which is defined as:

$$\text{tri}(x) = \begin{cases} 0 & |x| \geq x_m \\ 1 - |x|/x_m & |x| < x_m \end{cases}$$

However, there are still discontinuities in tri(x) at $x = 0$ and at $x = \pm x_m$. The Fourier transform of tri(x) is

$$\begin{aligned} \text{F.T.}[\text{tri}(x)] &= \int_{-\infty}^{\infty} \text{tri}(x) e^{2\pi i \bar{\nu} x} dx \\ &= \int_{-x_m}^{x_m} \left(1 - \frac{|x|}{x_m}\right) e^{2\pi i \bar{\nu} x} dx \\ &= \int_{-x_m}^{x_m} \cos(2\pi\bar{\nu}x) dx + i \int_{-x_m}^{x_m} \sin(2\pi\bar{\nu}x) dx \\ &\quad -\frac{1}{x_m} \int_{-x_m}^{x_m} |x| \cos(2\pi\bar{\nu}x) dx - \frac{i}{x_m} \int_{-x_m}^{x_m} |x| \sin(2\pi\bar{\nu}x) dx \end{aligned} \tag{38}$$

since $\sin(2\pi\bar{\nu}x)$ and $|x|\sin(2\pi\bar{\nu}x)$ are odd functions, then the integrals are identically zero, and thus Eq. 38 reduces to two terms:

$$= \frac{2\sin(2\pi\bar{\nu}x_m)}{2\pi\bar{\nu}} - \frac{2}{x_m}\int_0^{x_m} x\cos(2\pi\bar{\nu}x)dx$$

From a general calculus theorem, recall that

$$\int_a^b f(x)g(x)dx = \left[f(x)\int_0^x g(y)dy\right]_a^b - \int_a^b \frac{\partial f(x)}{\partial x}\left[\int_0^x g(y)dy\right]dx$$

then Eq. 38 becomes

$$\begin{aligned}
&= \frac{2\sin(2\pi\bar{\nu}x_m)}{2\pi\bar{\nu}} - \frac{2}{x_m}\left\{\left[\frac{x\sin(2\pi\bar{\nu}x)}{2\pi\bar{\nu}}\right]_0^{x_m} - \int_0^{x_m}\frac{\sin(2\pi\bar{\nu}x)}{2\pi\bar{\nu}}dx\right\} \\
&= \frac{2\sin(2\pi\bar{\nu}x_m)}{2\pi\bar{\nu}} - \frac{2}{x_m}\left\{\frac{x_m\sin(2\pi\bar{\nu}x_m)}{2\pi\bar{\nu}} + \left[\frac{\cos(2\pi\bar{\nu}x)}{(2\pi\bar{\nu})^2}\right]_0^{x_m}\right\} \\
&= -\frac{2}{x_m}\left[\frac{\cos(2\pi\bar{\nu}x_m)-1}{(2\pi\bar{\nu})^2}\right] \\
&= \frac{2}{x_m}\left[\frac{2\sin^2(\pi\bar{\nu}x_m)}{(2\pi\bar{\nu})^2}\right] \\
&= \frac{x_m\sin^2(\pi\bar{\nu}x_m)}{(\pi\bar{\nu}x_m)^2} \\
&= x_m\mathrm{sinc}^2(\pi\bar{\nu}x_m) \qquad (39)
\end{aligned}$$

The Fourier transform of $\mathrm{tri}(x)$ is shown in Fig. 7. Notice the absence of negative side lobes, the small size of the first positive lobes and the increase in the line width. Once again, a monochromatic line $\bar{\nu}$ would give a spectrum given by

$$\begin{aligned}
I(\bar{\nu}) &= I(\bar{\nu}_1) * \mathrm{ILS} \\
&= I(\bar{\nu}_1)x_m\mathrm{sinc}^2(\pi\bar{\nu}x_m). \qquad (40)
\end{aligned}$$

1.5.1 Resolution revisited

If we used the previous definition of resolution, the we would now have

$$\delta_{\bar{\nu}} = \frac{2}{x_m}$$

However, one normally adopts the Rayleigh criterion when attempting to resolve two close lines, which is obtained when when the first zero of one line falls upon the maximum of

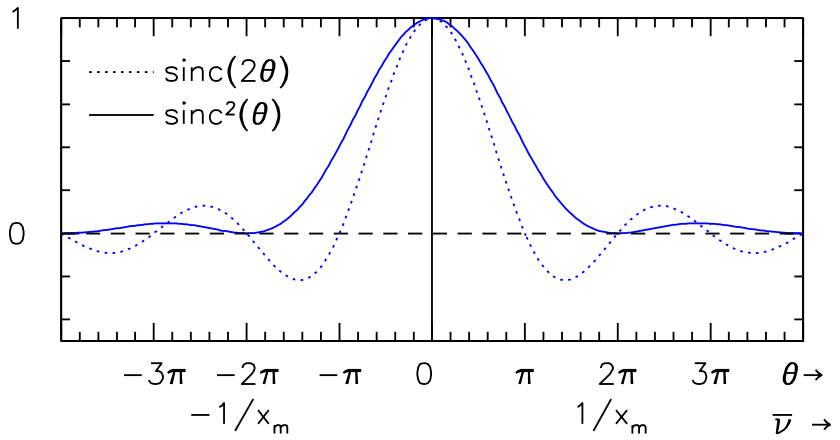

Figure 7: A comparison of the Fourier transforms of the rectangular and triangular aperture functions, $\mathrm{sinc}(2\theta)$ and $\mathrm{sinc}^2(\theta)$ respectively. Note that the Fourier transform of the triangular aperture function has much smaller side lobes, but is broader than the Fourier transform of the rectangular aperture.

the other line. When this condition is achieved, the dip between the two lines represents 22% of their maxima. (It should be noted that this assumes that the lines are of equal widths and strengths.) Thus, once again we have that the resolution is given by

$$\delta_{\bar{\nu}} = \frac{1}{x_m}.$$

There are many different kinds of apodisation functions, having a varying widths and side lobes. A function that has commonly been used is the Happ-Genzel function

$$W(x) = 0.54 + 0.46 \cos\left(\frac{\pi x}{x_m}\right). \tag{41}$$

The Fourier transform of the Happ-Genzel function is

$$\mathrm{F.T.}[W(x)] = \frac{\sin(2\pi\bar{\nu}x_m)}{2\pi}\left[\frac{1.08}{\bar{\nu}} + \frac{0.46}{x_m/w - \bar{\nu}} - \frac{0.46}{x_m/2 + \bar{\nu}}\right]. \tag{42}$$

A comparison of the Triangular and Happ-Genzel apodisation functions is shown in Figure 8. While the full width at half maximum for the two functions is about the same, the side lobes are almost totally absent in the Happ-Genzel function. In general, we will be using either three or four-term Blackwood-Harris apodisation functions, which have slightly narrower line shapes and very small side lobes.

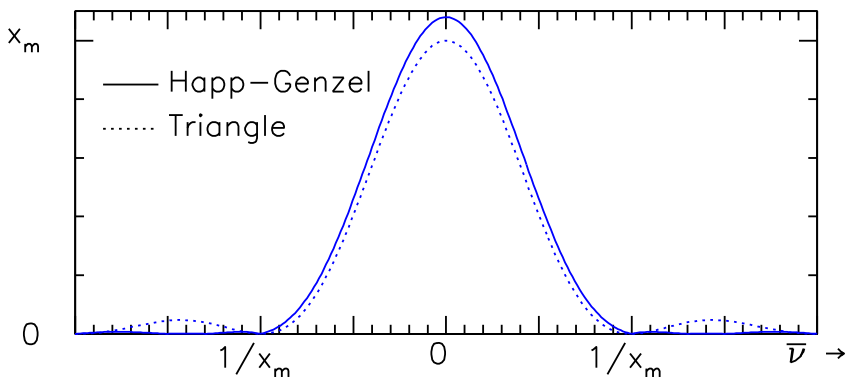

Figure 8: A comparison of the Fourier transforms of the Triangular and Happ-Genzel aperture functions. Note that the side lobes of the Happ-Genzel function are much smaller than those of the triangular apodisation function.

1.6 Sampling interval

The data has to bee digitized for the Cooley-Tukey fast Fourier transform algorithm in equal increments of path difference Δx. In many early instruments, the data was collected by a "step and integrate" method. Later instruments, such as the Bruker IFS113, adopted a "rapid scan" technique where the infrared radiation is modulated (typically in the kHz frequency range), and many interferograms are taken and averaged. This technique is generally superior to the step-and-integrate method.

The disadvantage of digitizing data in equal increments is the loss of symmetry in the interferogram if the zero-path difference is not sampled and the subsequent inability to detect spurious noise.

1.6.1 The Shah function

The sampled interferogram $F_s(x)$ is related to the complete interferogram $F_c(x) = [I(x) - I(\infty)]_c$ by:

$$F_s(x) = \text{⫚}\left(\frac{x}{\Delta x}\right) F_c(x) \tag{43}$$

where ⫚ (x) is a "combing" function, or Shah function defined by

$$\text{⫚}(x) = \sum_{-\infty}^{\infty} \delta(x-n) \tag{44}$$

where $\delta(x-n)$ is a Dirac delta function, and n is an integer. Thus, from Eq. 44 the Shah function allows only non-zero value for integers (both positive and negative). Thus, in

Eq. 43 the Shah function will allow non-zero value for

$$x = 0, \pm\Delta x, \pm 2\Delta x, \cdots, \pm n\Delta x, \cdots$$

Before proceeding, consider some of the properties of the Shah function. It is periodic (since the limits run from $-\infty$ to ∞)

$$\text{⫛}\,(x+m) = \text{⫛}\,(x). \tag{45}$$

We may also derive a scaling rule for the Shah function. Suppose one has

$$\text{⫛}\,(ax) = \sum_{n=-\infty}^{\infty} \delta(ax - n) \tag{46}$$

we would like to change the variable from $ax - n$ to $x - n/a$. If we consider the fitting property of the delta function, then

$$\int_{-\infty}^{\infty} \delta\left(x - \frac{n}{a}\right) f(x)dx = f\left(\frac{n}{a}\right) \tag{47}$$

and

$$\begin{aligned} \int_{-\infty}^{\infty} \delta(ax - n) f(x)dx &= \frac{1}{|a|}\int_{-\infty}^{\infty} \delta(y) f\left(\frac{y+n}{a}\right) dy \\ &= \frac{1}{|a|} f\left(\frac{n}{a}\right); y = ax - n. \end{aligned} \tag{48}$$

Comparing Eqs. 47 and 48 one has

$$\delta(ax - n) = \frac{1}{|a|}\delta\left(x - \frac{n}{a}\right) \tag{49}$$

thus

$$\text{⫛}\,(ax) = \frac{1}{|a|}\sum_{n=-\infty}^{\infty} \delta\left[x - \left(\frac{n}{a}\right)\right]. \tag{50}$$

We need to know what the effect of the Fourier transform is upon the Shah function.

$$\text{F.T.}[\text{⫛}\,(ax)] = \frac{1}{|a|}\sum_{n=-\infty}^{\infty}\int_{-\infty}^{\infty} \delta\left(x - \frac{n}{a}\right) e^{2\pi i\bar{\nu}x} dx \tag{51}$$

using the sifting property of the δ function gives that

$$\text{F.T.}[\text{⫛}\,(ax)] = \frac{1}{|a|}\sum_{n=-\infty}^{\infty} e^{2\pi i\bar{\nu}n/a} \tag{52}$$

$$= \frac{1}{|a|}\left\{\sum_{-\infty}^{\infty} \cos\left[2\pi\left(\frac{\bar{\nu}}{a}\right)n\right] + i\sum_{-\infty}^{\infty} \sin\left[2\pi\left(\frac{\bar{\nu}}{a}\right)n\right]\right\}. \tag{53}$$

In the cosine summation, whenever $\bar{\nu}/a \neq$ an integer value, the cosines will add randomly to zero. However, when $\bar{\nu}/a =$ an integer, then we get an infinite number of unities adding together. This is the definition of a δ function. Therefore,

$$\text{F.T.}[\text{⫛}\,(ax)] = \frac{1}{|a|}\sum_{n=-\infty}^{\infty}\delta\left[\left(\frac{\bar{\nu}}{a}\right) - n\right] \tag{54}$$

and

$$\text{F.T.}[\text{⫛}\,(ax)] = \frac{1}{|a|}\,\text{⫛}\left(\frac{\bar{\nu}}{a}\right). \tag{55}$$

The Fourier transform of the Shah function is another Shah function that is reciprocal to the first.

Returning to the spectrum

$$I_s(\bar{\nu}) = \text{F.T.}\,[F_s(x)] \tag{56}$$

and

$$I_c(\bar{\nu}) = \text{F.T.}\,[F_c(x)] \tag{57}$$

then

$$\begin{aligned}
I_s(\bar{\nu}) &= \text{F.T.}\left[\text{⫛}\left(\frac{x}{\Delta x}\right)F_c(x)\right] \quad [\text{from (48)}] && (58)\\
&= \text{F.T.}\left[\text{⫛}\left(\frac{x}{\Delta x}\right)\right] * I_c(\bar{\nu}) && (59)\\
&= \Delta x\,\text{⫛}\,(\bar{\nu}\Delta x) * I_c(\bar{\nu}) \qquad [\text{from (61)}] && (60)\\
&= \Delta x\sum_{n=-\infty}^{\infty}\delta(\bar{\nu}\Delta x - n) * I_c(\bar{\nu}) \quad [\text{from (49)}] && (61)\\
&= \sum_{n=-\infty}^{\infty}\delta\left(\bar{\nu} - \frac{n}{\Delta x}\right) * I_c(\bar{\nu}) \quad [\text{from (55)}] && (62)\\
&= \sum_{n=-\infty}^{\infty} I_c\left(\bar{\nu} - \frac{n}{\Delta x}\right) && (63)
\end{aligned}$$

so that we finally arrive at

$$I_s(\bar{\nu}) = \sum_{n=-\infty}^{\infty} I_c(\bar{\nu} - n\Delta\bar{\nu}) \tag{64}$$

where

$$\Delta\bar{\nu} = \frac{1}{\Delta x}. \tag{65}$$

Table 1: The minimum sampling interval required to prevent aliasing for the wave number range from $0 \rightarrow \bar{\nu}_{max}$ in a Michelson interferometer.

$\bar{\nu}_{max}$ (cm^{-1})	Δx (μm)
2000	2.5
1000	5
500	10
250	20
125	40
62.5	80

Thus, when transforming the sampled interferogram, we get an infinite number of complete spectra, each starting at $n\Delta\bar{\nu}$. The transformed spectra are actually the sum of the spectra for the positive frequencies and those of the negative frequencies from an adjacent spectra. Incorrect choices of a sampling frequency can lead to large contributions to distortions of the spectra. This is called "aliasing" or "false energies". In order to avoid this, one must make $\Delta\bar{\nu}$ large enough so that the maximum frequency contribution of the positive $\bar{\nu}$ spectrum does not overlap with the negative $\bar{\nu}$ spectrum. This may be accomplished by requiring that

$$\Delta\bar{\nu} \geq 2\bar{\nu}_{max} \tag{66}$$

or

$$\Delta x \leq \frac{1}{2\bar{\nu}_{max}}. \tag{67}$$

In term of wave number regions, this results in the following conditions: Another way of seeing the condition that $\Delta x \leq 1/2\bar{\nu}_{max}$ is that $\Delta x \leq \lambda_{min}/2$, which means that one must sample at least every twice in every cycle of the smallest wave length of radiation in the interferogram (this is just the Nyquist frequency from information theory). Having chosen $\bar{\nu}_{max}$, and found the appropriate Δx, one must make certain that there is no radiation with $\bar{\nu} > \bar{\nu}_{max}$ by the use of optical filters. The theory and results ere are the same as found in x-ray and electron diffraction in solids, where atoms are discrete, regularly spaced points.

1.7 Felgett advantage ("Multiplex")

Felgett submitted his dissertation to Cambridge in 1951, and was the first person to transform interferograms numerically. Shortly after this, Jacquinot stated his throughput advantage. The Felgett advantage is realized in the following way — suppose one is

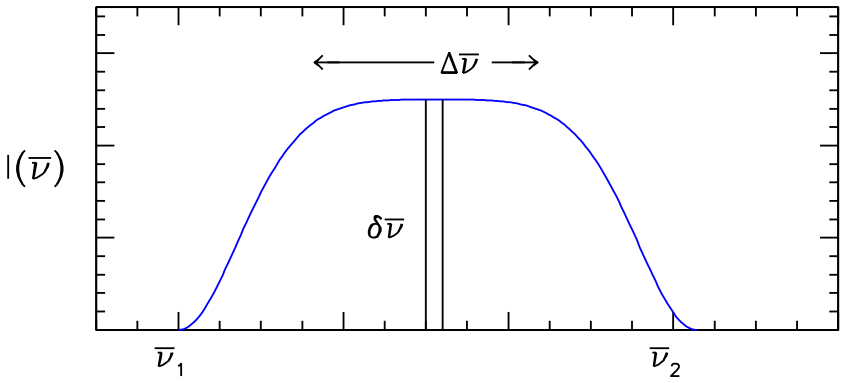

Figure 9: An arbitrary spectrum over an interval $\bar{\nu}_1$ and $\bar{\nu}_2$ ($\Delta\bar{\nu}$) to be measured with resolution $\delta\bar{\nu}$.

interested in measuring a spectrum of width $\Delta\bar{\nu}$ between $\bar{\nu}_1$ and $\bar{\nu}_2$ with resolution $\delta\bar{\nu}$, as shown in Fig. 9. The number of "elements", M is then given by:

$$M = \frac{\Delta\bar{\nu}}{\delta\bar{\nu}}. \tag{68}$$

If a grating or a prism instrument is being used, then each small band of width $\delta\bar{\nu}$, or element, is observed individually and for a time T/M, there T is the observed time for the entire spectrum.

In the infrared region the noise is due mainly to thermal and current contributions; it is independent of signal level. This is not the case in the visible region, where the uncertainty comes primarily from photon noise (the noise from the random counting of photons, which is simply proportion to the square root of the number of photons). In the infrared region, the noise, N, is then proportional to $\sqrt{T/M}$ in an element of width $\delta\bar{\nu}$. It follows that:

$$\left(\frac{S}{N}\right)_{\text{GRT}} \propto \frac{(T/M)}{\sqrt{T/M}} = \sqrt{T/M} \tag{69}$$

For an interferometer, however, the signal from all of the elements is received at the same time, thus the signal in an element is $\propto T$. Again, if the noise is random and independent of signal level then the noise $\propto \sqrt{T}$. Thus, the signal to noise in an interferometer is:

$$\left(\frac{S}{N}\right)_{\text{INT}} \propto \frac{T}{\sqrt{T}} = \sqrt{T} \tag{70}$$

The Felgett advantage of an interferometer over a grating instrument is then:

$$\frac{(S/N)_{\text{INT}}}{(S/N)_{\text{GRT}}} = \frac{\sqrt{T}}{\sqrt{T/M}} = \sqrt{M}. \tag{71}$$

For instance, for $\Delta\bar{\nu}$ from 200 to 1000 cm^{-1} with a resolution of 1 cm^{-1}, a S/N advantage of $\sqrt{800} \sim 28$ is realized; if a run takes 1 hour with the interferometer, an equivalent run on a grating instrument would have taken 800 hours! However, it should be noted that this advantage is lost in the visible region.

1.8 Relating (S/N) in the interferogram to (S/N) in the spectrum

Assume that the interferometer gives an interferogram that is composed of a noiseless interferogram plus random detector noise; the noise will be evident in the tails of the interferogram where the signal modulations are small. The RMS noise is given by:

$$\sigma_N = \sqrt{\overline{N(x)^2}} \tag{72}$$

which can be estimated by looking at the interferogram. The $(S/N)_{\text{IFG}}$ can be defined (and measured) as

$$\left(\frac{S}{N}\right)_{\text{IFG}} = \frac{I(0) - I(\infty)}{\sigma_N} \tag{73}$$

How will this transform into (S/N) of the interferometer spectrum where

$$\left(\frac{S}{N}\right)_{\text{SPT}} \propto T^{1/2} \tag{74}$$

in an element of width $\delta\bar{\nu}$. However, the interferogram contains all M elements simultaneously, thus the signal is proportional to MT and the noise is proportional to $\sqrt{MT}$. Thus, the signal-to-noise in the interferogram is

$$\left(\frac{S}{N}\right)_{\text{IFG}} \propto \frac{MT}{\sqrt{MT}} = \sqrt{MT} \tag{75}$$

Thus, the (S/N) in the spectrum divided by the (S/N) in the interferogram is

$$\begin{aligned} \left(\frac{S}{N}\right)_{\text{SPT}} \Big/ \left(\frac{S}{N}\right)_{\text{IFG}} = \frac{T^{1/2}}{(MT)^{1/2}} &= \frac{1}{M^{1/2}} \\ &= \sqrt{\frac{\delta\bar{\nu}}{\Delta\bar{\nu}}} \end{aligned} \tag{76}$$

with a low-pass filter, $\Delta\bar{\nu} = \bar{\nu}_{\max}$, thus

$$\sqrt{\frac{\delta\bar{\nu}}{\Delta\bar{\nu}}} = \sqrt{\frac{\text{Resolution}}{\bar{\nu}_{\max}}}. \tag{77}$$

If $\bar{\nu}_{\max} = 1000$ cm^{-1} with a resolution of $\delta\bar{\nu} = 10$ cm^{-1}, then

$$\left(\frac{S}{N}\right)_{\text{SPT}} / \left(\frac{S}{N}\right)_{\text{IFG}} = \sqrt{\frac{10}{1000}} = \frac{1}{10}$$

thus, 1% noise in the interferogram yields 10% noise in the spectrum. For the measurement of a reasonably narrow vibration in the terahertz range, if $\bar{\nu}_{\max} = 60$ cm^{-1} with a resolution of $\delta\bar{\nu} = 0.1$ cm^{-1}, then

$$\left(\frac{S}{N}\right)_{\text{SPT}} / \left(\frac{S}{N}\right)_{\text{IFG}} = \sqrt{\frac{1}{600}} = \frac{1}{25}$$

if 10% noise is acceptable in the spectrum, then we need a signal-to-noise of 250 for the interferogram.

2 Instrumentation

2.1 Self-supporting dielectric beam splitters

Most beam splitters are mylar (polyethylene teraphalate) of various thicknesses; 3 μm (12 G), 6 μm (25 G), 12 μm (50 G), up to 100 μm (400 G). Other beamsplitter materials, such as polycarbonate my also be used, in addition to wire-grid beam splitters.

The transmitted radiation through the interferometer depends on the product of the reflected intensity R_0, and the transmitted intensity T_0. The intensity from each beam reaching the detector, neglecting the modulation from the optical path difference in the two arms of the interferometer is simply R_0T_0, yielding a total of $2R_0T_0$. From $R_0+T_0 = 1$, then one can optimize the signal reaching the detector, and find a maximum efficiency when $R_0 = T_0 = 0.5$ (one half of the signal returns to the source). It should be noted that some instruments such as the lamellar grating interferometer return nothing and are 100 % efficient. We will define the relative efficiency (RE) of our beam splitter as:

$$\text{R.E.} = \frac{2R_0T_0}{(2R_0T_0)_{ideal}} = 4R_0T_0 \tag{78}$$

Unfortunately, the relative efficiency is often considerably less than unity due to $R_0 < 0.5$, R_0 and T_0 depend on the polarization, and the relative efficiency depends on frequency.

2.1.1 Efficiency of a dielectric beamsplitter with frequency

The variation of efficiency with $\bar{\nu}$ is known as "interference fringes", "channeled spectra", "dielectric resonances", of "Fabry-Perot fringes". Consider the plane waves incident on a non-absorbing, parallel-sided sheet of dielectric of thickness d, with amplitude a. We define the following amplitude coefficients:

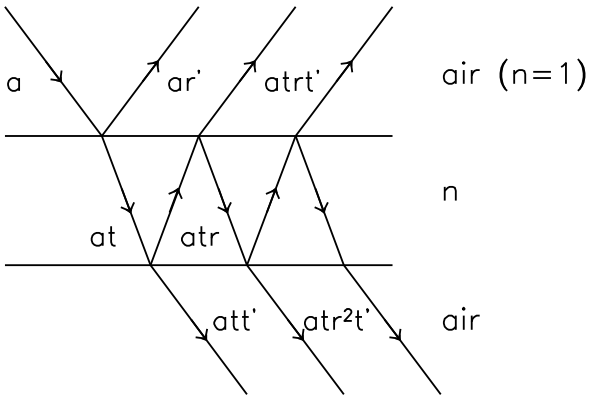

Figure 10: The reflected and transmitted rays at the front and back surfaces of a thin non-absorbing dielectric film of thickness d and refractive index n in air.

t	transmission from air to dielectric
t'	transmission from dielectric to air
r	reflection at the dielectric to air interface
r'	reflection at the air to dielectric interface

This is shown schematically in Fig. 10. The transmitted amplitude will therefore be given by:

$$Ae^{i\theta} = att' + att'r^2e^{i\delta} + att'r^4e^{i2\delta} + \cdots , \tag{79}$$

where δ is the change in the phase between two adjacent emerging rays. From the Stokes relation

$$tt' = 1 - r^2 \tag{80}$$

this expression can be rewritten as

$$Ae^{i\theta} = a(1-r^2)(1 + re^{i\delta} + r^4e^{i2\delta} + \cdots) \tag{81}$$

which sums to

$$Ae^{i\theta} = \frac{a(1-r^2)}{1 - r^2e^{i\delta}}. \tag{82}$$

The transmitted intensity is $T_0 = A^2 = Ae^{i\theta}Ae^{-i\theta}$. Thus

$$\begin{aligned} T_0 &= \frac{a^2(1-r^2)^2}{(1-r^2e^{i\delta})(1-r^2e^{-i\delta})} \\ &= \frac{a^2(1-r^2)^2}{1 + r^4 - r^2(e^{i\delta} + e^{-i\delta})} \\ &= \frac{(1-r^2)^2}{1 + [2r/(1-r^2)]^2 \sin^2(\delta/2)} \end{aligned} \tag{83}$$

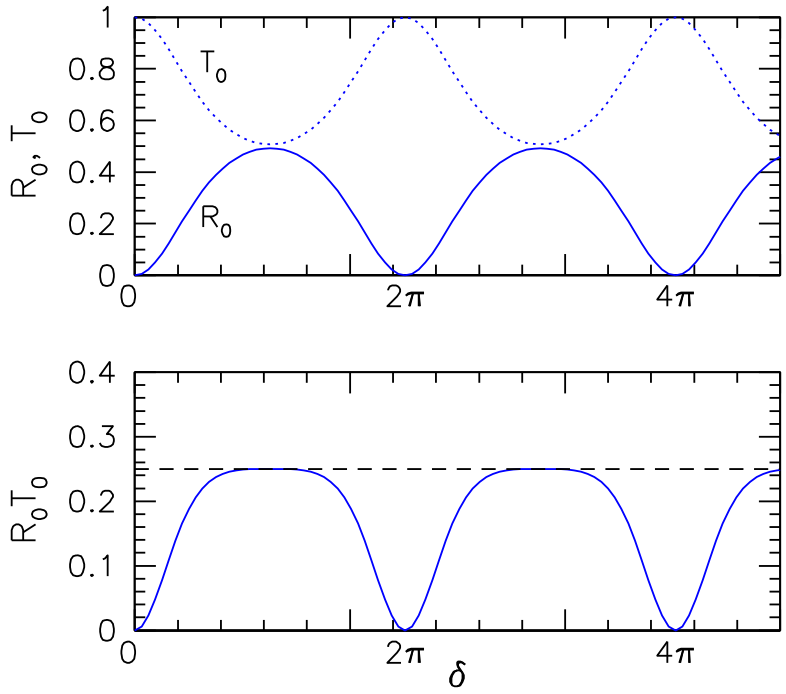

Figure 11: Upper panel: the variation of R_0 (solid line) and T_0 (dotted line) with the phase difference δ for $r = 0.41$ ($R = 0.16$); note that $R_0 + T_0 = 1$. Lower panel: the variation of R_0T_0 with δ.

Using the trigonometric identity $\cos\delta = 1 - 2\sin^2(\delta/2)$ and $R = rr^*$, then T_0 and R_0 can be written as:

$$T_0 = \frac{(1-R)^2}{1 + R^2 - 2R\cos\delta} \tag{84}$$

and

$$R_0 = \frac{2R^2(1-\cos\delta)}{1 + R^2 - 2R\cos\delta}. \tag{85}$$

The variation of R_0 and T_0 with δ is shown in Fig. 13.

This is the familiar Fabry-Perot fringe pattern, normally called channeled spectra when one encounters it due to a filter or a window, etc., with parallel faces somewhere in the optical path. One chooses the thickness of the beamsplitter material so that the wavenumber region of interest is in the first lobe.

2.1.2 Relating δ to $\bar{\nu}$

For an angle of incidence $\theta = 45°$, the optical path difference between emerging rays in a film of thickness d with refractive index n is $2ny - z = 2ny - 2x\cos(45°)$; here $x = d\tan\phi$

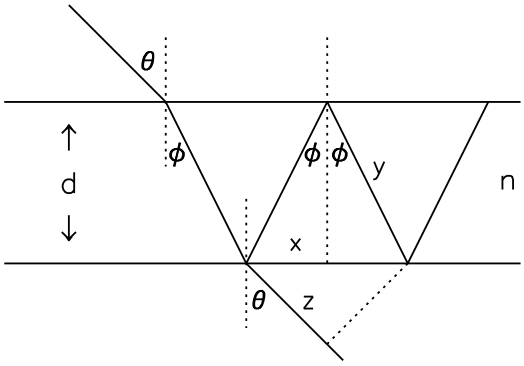

Figure 12: The optical path difference between two rays emerging from the back of a thin dielectric film of thickness d and refractive index n.

and $y = d/\cos\phi$, as illustrated in Fig. 12 . Therefore, the optical path difference may be written as $2nd/\cos\phi - 2d\tan\phi\cos(45°)$. Given that the film is in air with an index of $n = 1$, then from Snell's law $n\sin\phi = \sin\theta$; the optical path distance (OPD) is then

$$\begin{aligned} \text{OPD} &= 2nd\left(\frac{1}{\cos\phi} - \frac{\sin^2\phi}{\cos\phi}\right) && (86) \\ &= 2nd\cos\phi. && (87) \end{aligned}$$

This is similar to a previously obtained result, which I may not have actually talked about yet. Expressing ϕ in terms of the refractive index n,

$$\cos\phi = \sqrt{1-\sin^2\phi} = \sqrt{1 - \frac{\sin^2(45°)}{n^2}} = \sqrt{1 - \frac{1}{2n^2}}$$

For a maximum in the beam splitter efficiency, we have that

$$\frac{\delta}{2} = \left(n - \frac{1}{2}\right)\pi, \qquad n = 1, 2, 3, \cdots \tag{88}$$

which can be related to the frequency by $2\pi/\lambda \cdot \text{OPD}/2 = (n - 1/2)\pi$, which gives

$$\bar{\nu} = \frac{\left(n - \frac{1}{2}\right)}{2nd\left(1 - \frac{1}{2n^2}\right)^{1/2}} \tag{89}$$

for a maximum, and

$$\bar{\nu} = \frac{n}{2nd\left(1 - \frac{1}{2n^2}\right)^{1/2}} \tag{90}$$

for a zero. When the angle of incidence is normal to the surface, i.e. $\theta = \phi = 90°$, then one obtains channeled spectra whose separation $\Delta\bar{\nu}$ is given by

$$\Delta\bar{\nu} = \frac{1}{2nd}. \tag{91}$$

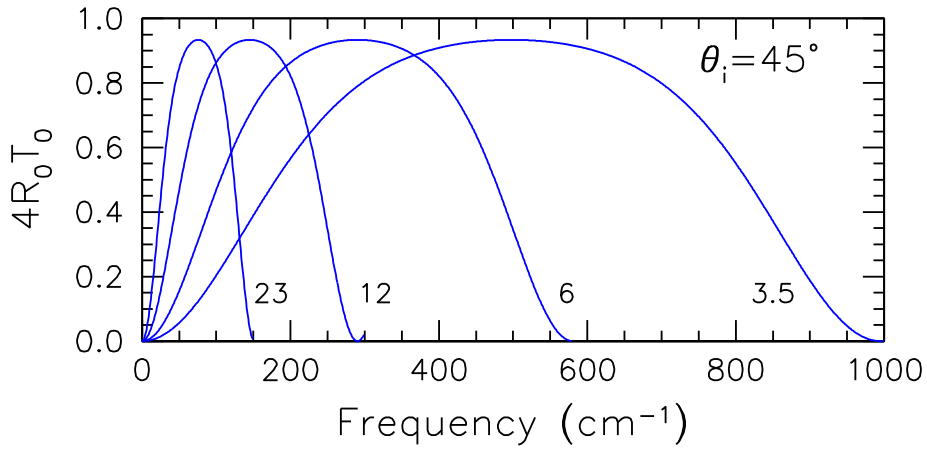

Figure 13: The beamsplitter efficiency versus frequency in a standard Michelson spectrometer ($\theta_i = 45°$) of 3.5, 6, 12 and 23 μm Mylar beam splitters as a function of frequency for s-polarized radiation.

2.2 Polarization in Mylar beam splitters

Radiation polarized with its electric field parallel to the plane of incidence is denoted by p, while radiation polarized with its electric field perpendicular to the plane of incidence is denoted by s. For any non-zero angle of incidence at the beamsplitter, the Fresnel equations for the reflectance for p- and s-polarized radiation have different forms

$$R_p = \frac{\tan^2(\theta_i - \theta_t)}{\tan^2(\theta_i + \theta_t)} \tag{92}$$

and

$$R_s = \frac{\sin^2(\theta_i - \theta_t)}{\sin^2(\theta_i + \theta_t)}, \tag{93}$$

where θ_i and θ_t are the angles of incidence and transmission, respectively, and are related by $n = \sin\theta_t / \sin\theta_t$. The refractive index of PET is $n \simeq 1.6$ and the index of absorption $k \approx 0$ over most of the far-infrared region. For an angle of incidence of $\theta_i = 45°$ found in

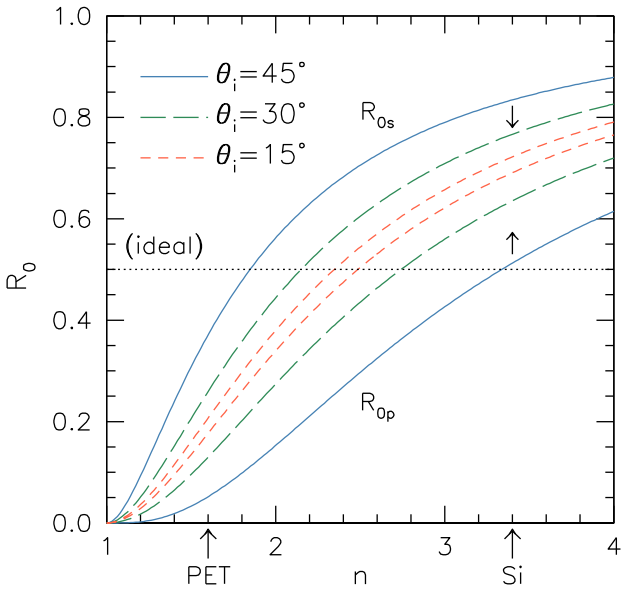

Figure 14: The variation of R_0 for s- and p-polarized radiation as a function of the refractive index for 45° (solid line), 30° (long dashed line) and 15° (short dashed line) angles of incidence. The values of the refractive index for both PET and Si are indicated. Note that for a high-index material such as Si, not only are the values for R_0 closer to the ideal value, but the difference between R_{0s} and R_{0p} is much smaller at a reduced angle of incidence (15°) than in a conventional Michelson spectrometer (45°).

a conventional Michelson interferometer, then $R_p = 0.133$, or about 1%, and $R_s = 0.155$, or about 11%, for the p and s polarizations, respectively. At the maximum in the beamsplitter response

$$T_0 = \left(\frac{1-R}{1+R}\right)^2 . \tag{94}$$

In the p polarization $T_{0p} = 0.9482$ and $R_{0p} = 1 - T_{0p} = 0.518$; $R_{0p}T_{0p} = 0.049$. We define the relative efficiency of a beamsplitter as $4T_0R_0 \approx 0.196$ or about 20% in this polarization. Similarly, for the s polarization $T_{0s} = 0.63$ and $R_{0s} = 0.37$, resulting in a relative efficiency of 93%. The Mylar beamsplitter efficiencies are listed below.

R_0	T_0	$4R_0T_0$	Polarization
0.52	0.95	0.20	p pol
0.37	0.62	0.93	s pol
0.29	0.71	0.83	unpol

Note that the relative efficiency of a beamsplitter will depend on its refractive index, as well as the angle of incidence, as illustrated in Fig. 14.

A Optical Conductivity

The relationship between the complex dielectric constant $\tilde{\epsilon} = \epsilon_1 + i\epsilon_2$ and the complex optical conductivity $\tilde{\sigma} = \sigma_1 + i\sigma_2$ is given by the following (SI) expression:

$$\tilde{\sigma} = i\epsilon_0\omega(1 - \tilde{\epsilon}) \tag{95}$$

where $\epsilon_0 = 8.854 \times 10^{-12}$ C^2/Nm^2 is the permittivity of free space. The real part of the optical conductivity is then

$$\sigma_1 = \epsilon_0\, \omega\epsilon_2. \tag{96}$$

However, we want the units for the conductivity to be in Ω^{-1}cm^{-1}. Examining the units of ϵ_0, and recalling that the units of resistance are $\Omega = \mathrm{m^2 kg/s\, C^2}$, we can write

$$\begin{aligned} \frac{\mathrm{C^2}}{\mathrm{N\, m^2}} &= \frac{\mathrm{C^2\, s^2}}{\mathrm{kg\, m^3}} \\ &= \left[\frac{\mathrm{s\, C^2}}{\mathrm{kg\, m^2}}\right]\frac{\mathrm{s}}{\mathrm{m}} \\ &= \Omega^{-1}\left(\frac{\mathrm{s}}{\mathrm{m}}\right). \end{aligned}$$

To remove the remaining (s/m), we multiply ϵ_0 by the speed of light c (m/s), so the units are now simply in Ω^{-1},

$$\begin{aligned} \epsilon_0 c &= (8.854 \times 10^{-12}\ \Omega^{-1}\,\mathrm{s/m})(2.997 \times 10^8\ \mathrm{m/s}) \\ &= 0.002654\ \Omega^{-1}. \end{aligned}$$

The fact that we are using an angular frequency adds a further factor of 2π, so that the final expression for the conductivity is then $\sigma_1(\omega) = (2\pi\epsilon_0 c)\,\omega\epsilon_2$. When the frequency is expressed in wave numbers (cm^{-1}), then $\sigma_1(\omega) = (2\pi\epsilon_0 c)\,\omega\epsilon_2$ has units of Ω^{-1}cm^{-1}; this can now be written as $\sigma_1(\omega) = 0.016678\,\omega\epsilon_2$ (Ω^{-1}cm^{-1}), or

$$\sigma_1(\omega) = \frac{\omega\epsilon_2}{59.96} \simeq \frac{\omega\epsilon_2}{60}\ \ (\Omega^{-1}\mathrm{cm}^{-1}). \tag{97}$$

As previously mentioned, ω is in cm^{-1}. This is the origin of the mysterious "1/60" term; it arises solely from a discussion of the units of the conductivity.